

## Combination of theoretical analysis and FTIR to study the photocurrent oscillation of Silicon in fluoride media

F. Yahyaoui<sup>1</sup>, L. Hlou<sup>2</sup>, M. Aggour<sup>1\*</sup>

<sup>1</sup>Département de Physique - LPMC - Faculté des Sciences, B.P 133, 14000, Kénitra – Maroc

<sup>2</sup>Département de Physique - LTNPSA - Faculté des Sciences B.P 133, 14000, Kénitra – Maroc

To deepening our knowledge of the behaviour of the silicon/electrolyte interface, a study of photocurrent oscillations on silicon in fluoride concentration  $c_F=0.033$  M is realized, and as a confirmation of the result the investigation is extrapolated to a variety of electrolyte compositions. The etch rates of anodic oxides in diluted fluoride solutions have been determined by using a new approach of the analysis of anodic current oscillations. The time dependent thickness of the anodic oxide has been measured by in-situ FTIR and can be simulated considering only the time dependent current and the etch rate.

### I. INTRODUCTION

The electrochemistry of silicon electrodes in fluoride media is of great interest in semiconductor processing, especially for devices preparation, due to control of the process by the current flux and/or the electrode potential. It is possible to modify the surface from rough and/or porous to smooth and vice versa under control of the potential and electrolyte composition. A simple change in pH may lead to atomically flat<sup>[1]</sup>, as well as rough silicon surfaces<sup>[2]</sup>. The most surprising observation of the behaviour of silicon-electrolyte interfaces is the photocurrent oscillations, which appear in a certain range (above ca. 3 V vs. SCE)<sup>[3]</sup> of anodic oxidation of silicon in diluted fluoride solutions. The appearance of oscillations on n-Si requires illumination while the phenomenon on p-Si also takes place in the dark, independently on crystal orientation and doping type.

This phenomenon has been studied extensively during the last decade. However, up to now, the mechanism of the anodic current oscillations is still under discussion. Changes in surface morphology of silicon oxide<sup>[4-7]</sup>, hole formation<sup>[5-7]</sup>, and variation of the amount of oxide<sup>[5-8]</sup> which is explained by non uniform anodic oxidation leading to photocurrent oscillation<sup>[5,6,9]</sup>, and passivation of the Si/SiO<sub>2</sub> interface and hydrogenated silicon surface<sup>[10,11]</sup>, are accompanying the oscillatory behaviour. Generally, most of the earlier studies, assumed that the oscillations in silicon/silicon oxide/electrolyte systems to be caused by a competition between oxide formation (connected with current flow) and dissolution (currentless).

The thickness of the anodic oxide layer and the relation between the etch rate and the rate of oxidation are quite important for better understanding of these processes.

The measurement of the etch rate of anodic oxides during anodic current oscillations is not simple because one has to measure the change of the amount of oxide and one has to consider the superposition of the oxidation and etch rates to get information about the etch rate. The thickness of the anodic oxides changes usually around 7 nm during the anodic current oscillations.

A theoretical model which might also describe consistently the microscopical physico-chemical events in the silicon/silicon oxide/electrolyte system has not yet been attempted, due to the complicated behaviour of chemical and physical process at surfaces.

In this paper, we present an in situ infrared spectroscopy study during photocurrent oscillations at +6V in 0.033 M (pH 3.8) in combination with a theoretical approach for the dissolution and formation of an oxide layer on silicon.

### II. EXPERIMENTAL

Phosphorus-doped n-Si(111) wafers (resistivity 20-35  $\Omega\text{cm}$ , float-zone purified) and boron-doped p-Si(100) wafers (resistivity 5 or 200  $\Omega\text{cm}$ ) served as working electrodes. For in-situ FTIR measurements, the samples were cut from a 0.5 mm thick polished wafer, shaped as 15-15 mm<sup>2</sup> platelets, and 45° bevelled for use as multiple-total-internal-reflection prisms. The platelets were provided with ohmic contact using 600°C evaporation of gold-antimony alloy and indium soldering on the gold pads.

The electrochemical cell was equipped with a platinum counter-electrode, and an Ag/AgCl (in saturated KCl) reference electrode.

The electrolytes were prepared from solutions of 1M HF, 1M N<sub>4</sub>HF, and 1M NH<sub>4</sub>Cl in ultra pure water<sup>[12]</sup>. The pH was adjusted by adding droplets of H<sub>2</sub>SO<sub>4</sub>.

The potential was stepped from the rest potential -0.5 V to +6 V under illumination (in the case of photocurrent oscillations on n-Si) and from -0.4 V to +6.9 V without illumination (in the case of anodic current oscillations on p-Si). In this cases, large current oscillations are triggered.

The anodic oxide was characterized by using IR vibrational spectroscopy in the potential difference mode (so-called Subtractively Normalized Fourier-Transform IR Spectroscopy- SNIFTIRS) at a BOMEM MB100 Fourier-Transform IR spectrometer<sup>/13/</sup> in the multiple internal reflection geometry (10 reflections). The IR electric field was parallel to the Si / electrolyte interface (s-polarisation). The reference spectrum was recorded for the hydrogenated silicon surface at  $V_0 \sim 0.5$  V. See for more details also Ref.<sup>/14/</sup>.

### III. RESULTS AND DISCUSSION

Figure 1 shows IR absorbance spectra during photocurrent oscillations at minimal and maximal thickness of the anodic oxide layer (0.033 M  $\text{NH}_4\text{F}$ , pH 3.8). The associated absorbance spectra contain the typical features of the Si-O-Si vibration modes around  $1100 \text{ cm}^{-1}$  and IR absorption at  $1700 \text{ cm}^{-1}$  and between  $3100$  and  $3500 \text{ cm}^{-1}$  which are related to the  $\text{H}_2\text{O}$  scissor and stretching modes, respectively<sup>/21/</sup>.

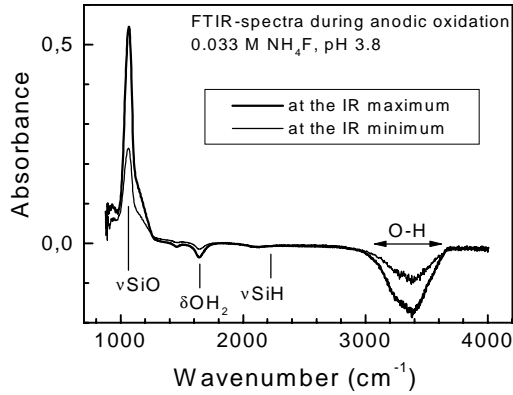


Figure.1: IR absorbance spectra at the maximum and at the minimum of the thickness of the anodic oxide during photocurrent oscillations for n-Si in 0.033 M  $\text{NH}_4\text{F}$ , pH 3.8.

The oxide thickness ( $d_{\text{ox}}$ ) can be calculated from the normalised FTIR spectra ( $\delta I/I$ ) integrated over the region of the Si-O-Si vibration modes by using the following equation:

$$d_{\text{ox}} = \frac{n_1 \cdot \cos \theta}{\pi^2 \cdot A_y \cdot C} \cdot \int \frac{\delta I}{I} d\sigma \quad (1)$$

where  $n_1$ ,  $\theta$ ,  $\sigma$ ,  $A_y$  and  $C$  are the refractive index of the ATR prism ( $n_1 = 3.42$ ), the incidence angle ( $\theta = 45^\circ$ ), the wave number, a numerical coefficient taking into account the geometry<sup>/19/</sup> ( $A_y = 2.32$ ) and a constant in the definition of the dielectric function ( $C = 1500$ <sup>/20/</sup>), respectively.

A typical example for the time dependence of photocurrent oscillations and of the respective thickness of the anodic oxide is presented in figure 2 for n-Si in 0.033 M  $\text{NH}_4\text{F}$  (pH 3.8). The oscillations are regular and the period is about 300 s at these conditions. The amplitude and the frequency of the photocurrent oscillations depend strongly on the composition of the electrolyte and on the applied potential<sup>/16/</sup>. The thickness of the anodic oxide layer ( $d_{\text{ox}}$ ) adopts a similar oscillation behaviour as the photocurrent, result which is already experimentally supplied by FTIR<sup>/15,18/</sup>.  $d_{\text{ox}}$  changes between 4 and 11 nm for the given electrolyte. There is a phase shift between the photocurrent maxima and the corresponding oxide thickness. Such phase shift has been also reported by Aggour et al.<sup>/16/</sup> and Chazalviel<sup>/18/</sup> et al. and has to do with the time dependent relation between the oxidation and etch rates.

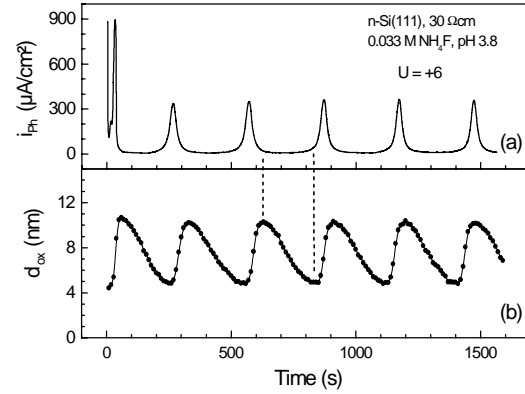


Figure.2: Time dependence of the photocurrent oscillations (a) and of the respective thickness of the anodic oxide (b) for n-Si in 0.033 M  $\text{NH}_4\text{F}$ , pH 3.8 at  $U = +6$  V.

We found that the current densities at which the maximal and minimal thickness of the anodic oxide layers ( $d_{\text{max}}$  and  $d_{\text{min}}$ , respectively) are reached, are identical. For this reason, a value of a current  $j_M$

$$j_M = j(d_{\text{max}}) = j(d_{\text{min}}) \quad (2)$$

can be defined independently of the concentration and of the pH of the diluted fluoride solution. As remark,

the value of  $j_M$  is practically equal to the average current density (for example, 56 and 60  $\mu\text{A}/\text{cm}^2$ , respectively, for 0.033 M  $\text{NH}_4\text{F}$ , pH 3.8 at +6 V). For this reason, the average current can be also used (instead of  $j_M$ ) in the following considerations.

The dependence of the maximal and minimal thickness of the anodic oxide and of the difference of both on the pH is given in figure 3 for n-Si in 0.033 M  $\text{NH}_4\text{F}$ . The value of  $d_{\text{max}}$  is about 8 nm and nearly constant for pH up to 3.0 and increases to 10-11 nm with increasing pH (pH changed up to 4.3). At the higher pH,  $d_{\text{max}}$  tends again to saturation. In difference to  $d_{\text{max}}$ , the value of  $d_{\text{min}}$  decreases with increasing pH while  $d_{\text{min}}$  tends to saturation for the lower pH and to a decrease for pH > 4.0. As result, the difference  $d_{\text{max}} - d_{\text{min}}$  increases continuously from about 1 nm at pH 2.5 to 7 nm at pH 4.0. The value of  $d_{\text{max}} - d_{\text{min}}$  increases with increasing pH and therefore with decreasing etch rate and saturates at lower etch rates. It would be interesting to carry out experiments in the range of very low etch rates (pH close to 5) to get more detailed information.

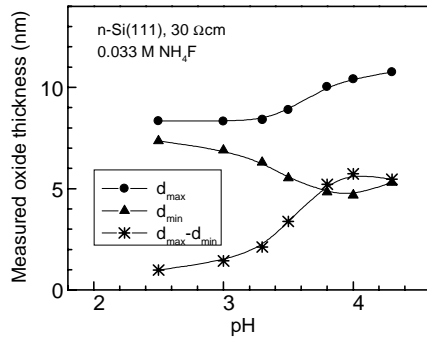


Figure.3: Dependence of the maximal and minimal thickness of the anodic oxide and of the difference of both on the pH for n-Si in 0.033 M  $\text{NH}_4\text{F}$ .

The change of the oxide thickness in time is given by the difference between the oxidation rate ( $K_{\text{ox}}$ ) and the etch rate of the anodic oxide ( $R$ ):

$$\frac{\partial d_{\text{ox}}}{\partial t} = K_{\text{ox}} - R \quad (3)$$

The etch and oxidation rates are equal at  $d_{\text{max}}$  and  $d_{\text{min}}$  (equation(2)). Oxide formation or etching predominate when  $j > j_M$  or  $j < j_M$ , respectively.

The density of the anodic current at a given time  $t$  is determined by the oxidation rate

$$j(t) = \alpha K_{\text{ox}}(t) = \frac{\delta Q(t)}{\delta t} \quad (4)$$

where  $\alpha$  and  $\delta Q(t)$  are a proportionality factor and the charge flown within the time interval  $\delta t$ . The flown charge normalized to the surface area is given by  $\delta Q(t) = 4 \cdot q \cdot \delta N(t)$ , where  $q = 1.6 \cdot 10^{-19}$  As and  $\delta N(t)$  is the amount of oxidized Si-atoms. The factor 4 appears due to the fact that 4 holes are consumed for the oxidation of a Si-atom in the overall oxidation reaction<sup>/17/</sup>. The amount of oxidized Si atoms determines the thickness of the oxide layer formed within  $\delta t$  ( $\delta d_{\text{ox}}(t)$ ) and it can be written:  $\delta N(t) = \rho \cdot N_A \cdot \delta d_{\text{ox}}(t) / M$  ( $M = 60$  g/mol - molar mass of  $\text{SiO}_2$ ,  $\rho = 2.2$  g/cm<sup>3</sup> - the specific gravity of  $\text{SiO}_2$  and  $N_A = 6.022 \cdot 10^{23}$  /mol - Avogadros number). Since  $K_{\text{ox}} = \delta d_{\text{ox}} / (t \delta t)$ , one will get  $\alpha = 4 \cdot q \cdot \rho \cdot N_A / M$  and therefore;

$$R = \alpha^{-1} j_M = \frac{M}{4 q \rho N_A} j_M \quad (5)$$

In the following, we will consider a constant etch rate  $R$  given by equation (5) independent of time and of  $d_{\text{ox}}$ . As remark, equation (5) corresponds in principle only to the etch rate at times when  $d_{\text{ox}} = d_{\text{min}}$  or  $d_{\text{ox}} = d_{\text{max}}$ . The thickness of the oxide layer at a given time  $t_{i+1}$  ( $d_{\text{ox}}(t_{i+1})$ ) is determined by the thickness of the oxide layer at a given earlier time  $t_i$  ( $d_{\text{ox}}(t_i)$ ) and by the integrated current density with respect to  $j_M$  which separates the regions where etching or oxide growth dominate (integral from  $t_i$  to  $t_{i+1}$ ):

$$d_{\text{ox}}(t_{i+1}) = d_{\text{ox}}(t_i) + \alpha^{-1} \cdot \int_{t_i}^{t_{i+1}} (j(t) - j_M) dt \quad (6)$$

An initial value  $d_{\text{ox}}(t_0)$  can be determined by FTIR. We point out that equation (6) implements a constant etch rate and that for this reason equation (6) can be used to prove this assumption by comparing the measured and calculated values of  $d_{\text{ox}}$ . Figure 4 shows an example for a time dependence of  $d_{\text{ox}}(t)$  (0.033 M  $\text{NH}_4\text{F}$ , pH 3.8,  $U = 6$  V) for simulation after equation (6) and for measured values. As expected, the simulated thickness of the anodic oxide adopts a similar oscillation behavior as the photocurrent (Fig.4a). The simulated and measured values of  $d_{\text{ox}}(t)$  are practically equal what gives evidence that  $R$  can be really assumed as constant for the given experimental conditions. This fact is not trivial since the microscopic structure of thin anodic oxides may depend on the thickness and therefore  $R$  would not be constant. Obviously, the thin anodic oxide layers are quite homogenous between 4 and 12 nm. Chazalviel et al. found some evidence for a time dependent etch rate<sup>/18/</sup>. Probably, the slight deviations between the simulated and measured values at lower oxide thickness are caused by changes in  $R$ .

A phase shift has been observed between the simulated and measured time dependencies of  $d_{ox}$  (see figure 4, the measured values are slightly retarded). This shows that the model of equation (6) is too simple for the exact description of  $d_{ox}(t)$ . For example, rates of transport through the thin anodic oxide layer should be taken into account for more sophisticated models.

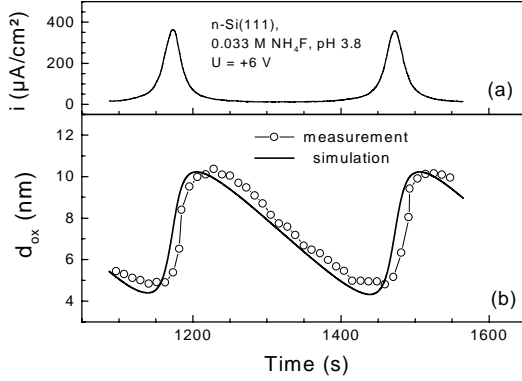
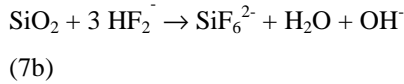
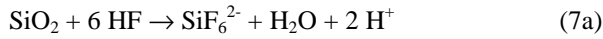


Figure 4: Time dependence of the photocurrent oscillations (a) and of the respective measured (circles) and simulated (line) thickness of the anodic oxide (b) for n-Si in 0.033 M  $\text{NH}_4\text{F}$ , pH 3.8 at  $U = +6$  V.

Equation (5) allows the experimental determination of the etch rate of anodic oxide as well as the oxidation rate (for the pH and the molarity considered) by measuring the time dependent anodic current. Eq.5 is valid not only for the photocurrent oscillations of n-Si also for the anodic current oscillations of p-Si.

Usually,  $\text{HF}$  and  $\text{HF}_2^-$  are considered to etch silicon oxides according to the following reaction equations:



The crucial importance of the pH of the solution for the etching of silicon oxides was demonstrated in earlier experiments<sup>22,23/</sup>. The influence of the pH on the chemical equilibrium in the electrolyte and therefore on the concentrations of the  $[\text{HF}]$  and  $[\text{HF}_2^-]$  components is evident<sup>24/</sup>:

$$k_1 [\text{HF}] = [\text{H}^+] [\text{F}^-] \text{ with } k_1 = 1.3 \times 10^{-3} \text{ mol/l} \quad (8a)$$

$$k_2 [\text{HF}_2^-] = [\text{HF}] [\text{F}^-] \text{ with } k_2 = 0.104 \text{ mol/l} \quad (8b)$$

The total concentration of fluor in the electrolyte ( $c_F$ ) is given by;

$$c_F = 2[\text{HF}_2^-] + [\text{HF}] + [\text{F}^-] \quad (9)$$

At low pH values (between 2 and 5), the etching occurs mainly by  $\text{HF}_2^-$ , but it becomes negligible for pH values exceeding 5.

Attempts have been made to separate the different reaction mechanisms, but none of the attempts so far have yielded a model which was valid for the whole range of HF concentrations. In fact, especially for the low concentrations, Judge<sup>25/</sup> was the first who proposed a qualitative description of the dissolution rate of a thermal oxide, based on two reactive species,  $\text{HF}_2^-$  and  $\text{HF}$ , where the former act four to five times faster than the later one:

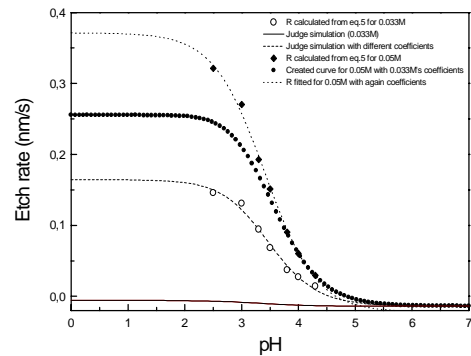
$$R = a [\text{HF}] + b [\text{HF}_2^-] + c \quad (10)$$

where a and b contain activation energy-type terms (at 25°C:  $a = 0.25$ ,  $b = 0.97$ , and  $c = -0.014^{25/}$  if the unit of R is nm/s).

In the aim to extract the etch rate of the anodic oxide, we achieve values of  $J_M$  from the photocurrent oscillations measured in  $c_F = 0.033$  M at different pH values (from pH 2.5 to pH 4.3). The data points shown in figure 5, acquired from Eq. 5 for 0.033M (open circle), have been fitted by Judge model in a wide pH range from 0 to 7 (solid line). With the given coefficients (above) Judge's formulae fails to adjust our acquired points from Eq.5, but it succeeded to improve the adaptation of our points with various coefficients. A good fitting (dashed line) is succeeded with:

$$a = 5.385 \pm 0.368, b = 33.361 \pm 10.867, \text{ and } c = -0.013 \pm 0.007$$

From this fitting, we see that the coefficient b can be determined only with large standard error, but the value



of c is almost in accordance with that given by Judge. To test the validity of the determined coefficients, the obtained fitting parameters will then be used to adjust the etch rate calculated as well as for the concentration 0.05M by using the Eq.5.

Figure 5: The etch rate calculated from Eq.5, for 0.033M(open circle), its curve- fitting by judge formulae with the given coefficients(solid circle), and with the found one (solid), the etch rate (from Eq.5) for 0.05M (diamond), with the found coefficients for 0.033M(dashed), and with another's coefficients(doted) as function of pH.

As can be seen from Fig. 5, if we keep the same coefficients found for 0.033M fixed, the adaptation for 0.05M (solid circle) exceeds all the data points(diamond). An almost good fit is obtained as when the fitting(doted) is done with;

$$a=7.870\pm0.284, b=28.103\pm5.883, \text{ and } c=-0.022\pm0.009.$$

Consequently judge model fails in our conditions, thus one needs to change the coefficients in passing from a concentration to the other.

Later, Kikuyama et .al<sup>[26]</sup>, found that etching of SiO<sub>2</sub> by HF<sub>2</sub><sup>-</sup> occurs according to the following relationship with R(HF<sub>2</sub><sup>-</sup>) in nm/s;

$$R = a[\text{HF}_2^-] + b[\text{HF}_2^-] \log\left(\frac{[\text{H}^+]}{[\text{HF}_2^-]}\right) \quad (11)$$

With a and b are two parameters dependent on the report of [H<sup>+</sup>] and [HF<sub>2</sub><sup>-</sup>] as;

$$a = 2.138, b = 0.648. \text{ when } \left(\frac{[\text{H}^+]}{[\text{HF}_2^-]}\right) \geq 2.10^{-2}.$$

They determined this relation in modified buffered HF at pH values  $\geq 2$ . This shows that in the etching reaction of HF<sub>2</sub><sup>-</sup> with SiO<sub>2</sub>, H<sup>+</sup> also play a role.

In our case  $\left(\frac{[\text{H}^+]}{[\text{HF}_2^-]}\right)$  ratio is always larger than 1, since;

$$[\text{H}^+] + [\text{NH}_4^+] = [\text{F}^-] + [\text{HF}_2^-] + [\text{OH}^-] + [\text{Cl}^-] \quad (12)$$

due to the charge neutrality.

Figure 6, shows the adjustment of the etch rate R calculated from Eq.5 with the formula proposed by kikuyama (Eq.11).

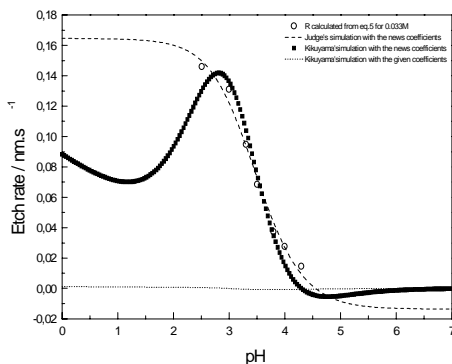


Fig. 6: The etch rate calculated from Eq.5(open circle), its curve- fitting by judge(solid), by Kikuyama with the given coefficients(cross), and the found coefficients (square) as function of pH, for  $c_F = 0.033\text{M}$

This model also not succeeded to adjust our points by considering the coefficients given by Kikuyama(doted line). In the object to try to perfect the adaptation by kikuyama's formulae, again coefficients are found by iteratif calculation,

$$a = 287.496 \pm 25.261 \text{ and } b = 47.210 \pm 6.105 \text{ (square).}$$

For Kikuyama model, the mechanism of why the H<sup>+</sup> ion concentration influence SiO<sub>2</sub> etching is changed at the  $\left(\frac{[\text{H}^+]}{[\text{HF}_2^-]}\right)$  ratio of  $2.10^{-2}$  was not justified, also from Eq.11 the etching rate depends mainly on the  $[\text{HF}_2^-]$  concentration which is clear for pH superior to 2.5, on the other hand the Kikuyama's model does not involve any contribution from HF, however it is necessary to take it into account, especially if pH < 2.5. In order to improve these formulae (Eqs.10 and 11), and optimize the conditions of parameters, from experimental points access to a more general expression of R in a large pH range [0-7] may be taken. For this fact, being based on formulae proposed by Judge<sup>[25]</sup> and the study of the others authors<sup>[26]</sup>, we have deduced that this multitude of formulae take account only a development of R in first order of concentration. None of these equation has given the good concordance with the obtained results, especially for pH larger than 2, in which the etching occurs mainly by the HF<sub>2</sub><sup>-</sup>.

However, we tried to find a formula which can satisfy our results by combination of Judge's model (Eq. 10) and that of Kikuyama (Eq.11), we found that the etch rate can best be described by the following equation;

$$R = c_F(a([\text{HF}] + [\text{HF}_2^-]) + b[\text{HF}_2^-] \log\left(\frac{[\text{H}^+]}{[\text{HF}_2^-]}\right)) \quad (13)$$

As can be seen, Eq.13 is a second-order equation in concentration, the dependence of the etching rate both of [HF] and  $[\text{HF}_2^-]$  concentrations is taking into account. The H<sup>+</sup> also play a role in the etching rate, but the functionality of [H<sup>+</sup>] is small, because it changes logarithmically. This relation (Eq.13) is valid for solutions where the

The calculation of R from the above relationship (Eq.13) has given the curve-fitting (solid) in Fig. 7, with adjustment parameters a and b given with their errors;

$$a = 158.843 \pm 5.207, b = 93.193 \pm 15.962.$$

The standard error on the coefficients is low, which means that the accuracy of the coefficients obtained is high.

therefore the given formulae have succeeded to have a good concordance.

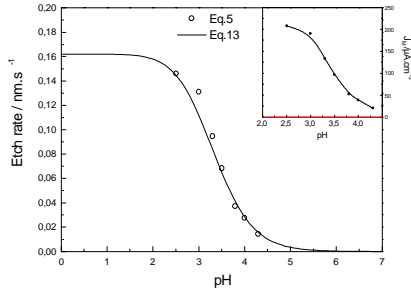


Figure. 7: The etch rate from Eq.5 (open circle), its curve- fitting by Eq.13 (solid) as function of pH, for  $c_F = 0.033M$

Furthermore, from Fig.4 if the current density undergoes a little change relatively to  $J_M$ , consequently also a local pH variation will take place. One can explain this such as, when oxide formation predominates, the current increases and therefore the pH decreases, whereas it increases when currentless etching prevails.

Since the etch rate depends on pH of the electrolyte, the etching process is therefore accelerated in the time range of highest current and delayed for low current densities.

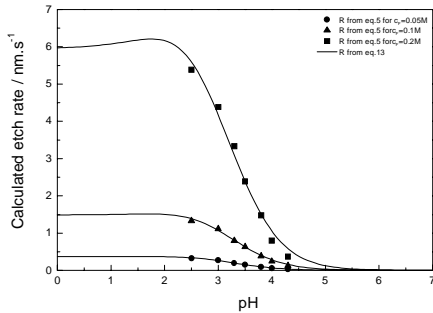


Fig. 8: The etch rate from Eq.5 (solid symbols), and its curve- fitting (solid) as function of pH, for  $c_F = 0.05 M$ ,  $c_F = 0.1 M$ , and  $c_F = 0.2 M$ .

To supplement our investigations, aiming to confirm the validity of our model, we also extended it to other concentrations namely;  $c_F = 0.05 M$ ,  $c_F = 0.1 M$  and  $0.2 M$ , the points data of the etch rate are calculated from the measured average photocurrent by Eq.5, and then fitted with the above relationship (Eq.13).

For each concentration  $c_F$ ,  $R$  as well as its curve-fitting are presented as a function of the pH in Fig. 8.

The fit is established for the same values of  $a$  and  $b$  obtained for  $c_F = 0.033 M$ . They are in good agreement with the experimental results.

Then we conclude that knowing the fluoride concentration  $c_F$ , and the pH of the used electrolyte, the etch rate can be determined by the equation presented above (Eq.13). Which is ascertained at least for the used electrolyte in this work.

## VI. Conclusion

Our study reveal that knowing the used electrolyte composition, one can anticipate the magnitudes and variations of some parameters, such as photocurrent, oxide thickness. A new approach for the determination of the etch rates and oxidation rates of thin anodic layers has been proposed on the basis of correlation between anodic current oscillations and the anodic oxide thickness in diluted fluoride solutions. The time dependent thickness can be well simulated by taking into account only the time dependent anodic current oscillations and a constant etch rate.

## Acknowledgement

The authors are grateful to Professor J.-N. Chazalviel and F. Ozanam, LPMC- Ecole Polytechnique, for IR-spectroscopy measurements.

## References

- [1]: G. S. Higashi, Y. J. Chabal, G. W. Trucks and K. Raghavachari, Appl. Phys. Lett., 56 (1990) 656.
- [2]: V. A. Burrows, Y. J. Chabal, G. S. Higashi, K. Raghavachari and S. B. Christman, Appl. Phys. Lett., 53 (1988) 998.
- [3]: D. R. Turner, J. Electrochem Soc., 105(1958) 402.
- [4]: J. Rappich, H. Jungblut, M. Aggour, and H.-J. Lewerenz, J. Electrochem. Soc. 141, L99 (1999).
- [5]: H.-J. Lewerenz, M. Aggour, J. Electroanal. Chem. 351, 159-168 (1993)
- [6]: M. Aggour, M. Giersig and H.-J. Lewerenz, J. Electroanal. Chem. 383, 67 (1995).
- [7]: J. Rappich, M. Aggour, S. Rauscher, H. Jungblut, and H.-J. Lewerenz, Surf. Sci. 335, 160(1995).
- [8]: O. Nast, S. Rauscher, H. Jungblut, and H.-J. Lewerenz, J. Electroanal. Chem. 422, 169-174(1998)
- [9]: F. Ozanam, and J.-N. Chazalviel, J. Electron Spectrosc. Relat. Phenom. 64/65, 395 (1993).
- [10]: J. Rappich, V. Y. Timoshenko, R. Würz, and T. Dittrich, Electrochim. Acta, (2000).
- [11]: S. Rauscher, T. Dittrich, M. Aggour, J. Rappich and H.-J. Lewerenz, Appl. Phys. Lett. 66, 3018 (1995).

- [12]: Hamdy. H. Hassan, PHD Thesis, University of Ain Shams, Egypt (1994).
- [13]: F. Ozanam, and J.-N. Chazalviel, Rev.Sci. Inst., 59(1988) 242.
- [14]: C. da Fonseca, F. Ozanam, J.-N. Chazalviel, Surf. Sci 365 (1996) 1-14
- [15]: H.-J. Lewerenz, J. Phys. Chem. B (1997), 101, 2421-2425
- [16]: F. Ozanam, J.-N. Chazalviel, A. Radi and M. Etman, Ber. Bunsenges. Phys. Chem. 95 (1991) 98.
- [17]: E. Duffek, E. Benjamini, and C. Mylroie, Electrochem. Technol. 3, 75 (1965)
- [18]: J.-N. Chazalviel, C. da Fonseca, and F. Ozanam, J. Electrochem. Soc., 145 (1998) 964-973.
- [19]: Y. Chabal, Surf. Sci. Rep., 8, 211(1988).
- [20]: C. T. Kirk, Phys. Rev. B, 38, 1255 (1988)
- [21]: Y. J. Chabal, S. B. Christman, Phys. Rev. B 29, 6974 (1984).
- [22]: H.-J. Lewerenz, Electrochim. Acta, 37, 847(1992).
- [23]: J. Stumper and H.-J. Lewerenz, J. Electroanal. Chem. Interfacial Electrochem., 274, 11 (1989)
- [24]: R. E. Mesmer and C. F. Baes, Inorg. Chem. 8, 618 (1969)
- [25]: J. S Judge, J. Electrochem. Soc., 118(1971)1772.
- [26]: H. Kikuyama, N. Miki, K. Saka, J. Takano, I. kawanabe, M. Miyashita and t. Ohmi, IEEE Trans. Semiconductor Manufacturing, Vol. 4, No.1, Feb. (1991).